ORGANIC PROCESS RESEARCH & DEVELOPMENT
OPR&D

pubs.acs.org/OPRD Article

Thermal Risk Analysis Based on Reaction Mechanism: Application to the 2,6-Diaminopyrazine-1-oxide Synthesis Process

Published as part of the Organic Process Research & Development joint virtual special issue "Process Safety from Bench to Pilot to Plant" in collaboration with ACS Chemical Health & Safety and Journal of Loss Prevention in the Process Industries.

Yuehua Li, Yang Wang, Longyu Liao, Zichao Guo,* Liping Chen, and Wenqian Wu

Cite This: *Org. Process Res. Dev.* 2021, 25, 849–857 Read Online

ACCESS | Metrics & More | Article Recommendations | Supporting Information

ABSTRACT: Thermal risk analysis is essential for the development of chemical reactions. This work should be carried out on the basis of a thorough comprehension of the reaction mechanism. In this article, the synthesis process for 2,6-diaminopyrazine-1-oxide (DAPO), an important intermediate in the synthesis of the famous explosive 2,6-diamino-3,5-dinitropyrazine-1-oxide (LLM-105), was employed to show the importance of understanding the reaction mechanism for thermal risk analysis. First, we investigated the reaction mechanism of DAPO synthesis. The reaction mechanism was divided into two stages on the basis of the amount of triethylamine dosed: the first half of triethylamine dosing and the second half of triethylamine dosing until the end of the reaction. Then the thermal properties of DAPO synthesis and the thermal stability of the materials involved were experimentally studied using a reaction calorimeter (RC1) and a differential scanning calorimeter (DSC), respectively. The results show that the temperature corresponding to the maximum reaction rate reached in a time of 24 h under adiabatic conditions (T_{D24}) is higher than the maximum temperature of the synthesis reaction (MTSR) for both of these stages, indicating that once cooling failure occurs, immediately stopping addition of triethylamine could prevent the occurrence of secondary decomposition.

KEYWORDS: *2,6-diaminopyrazine-1-oxide (DAPO), cyclization reaction, reaction mechanism, thermal risk assessment*

1. INTRODUCTION

2,6-Diamino-3,5-dinitropyrazine-1-oxide (LLM-105) is a highly heat-resistant explosive developed by the Livermore Energetic Materials Laboratory in the United States.[1−3] LLM-105's energy is 20% higher than that of trinitrotriaminobenzene (TATB), and it has relatively low sensitivity to impact, sparks, friction, and shock waves. It has shown certain application prospects in the fields of petroleum perforating bombs and boosters.[4−8]

To synthesize LLM-105, Bellamy[9−12] used 2,6-diaminopyrazine as the starting material to obtain the target product LLM-105 through a two-step process of oxidation and nitration. However, the side product of oxidation in this method has properties similar to those of the main product, which is not conducive to separation and purification, and the nitration reaction process is difficult to control. Another traditional synthesis method uses 2,6-dichloropyrazine as the starting material and completes it through a four-step reaction (two methoxyl oxidation, nitration, amination, and oxidation).[13] However, this process has the disadvantages of high cost and use of a highly corrosive material, namely, trifluoroacetic acid.[14]

Pagoria[15] used iminodiacetonitrile as the starting material to obtain LLM-105 through a three-step reaction of nitrosation, cyclization, and nitration (the synthesis route is illustrated in Figure 1). This synthesis route has the advantages of cheap and readily available raw materials, simple process steps, easy storage and use of intermediates, and high product purity. The cyclization reaction takes *N*-nitrosobis(cyanomethyl)amine (**1**) as the raw material to synthesize the intermediate 2,6-diaminopyrazine-1-oxide (DAPO). As one important step to synthesize LLM-105, several predecessors have conducted research on this process. Zhao[16] speculated about the cyclization reaction process of DAPO. Wang[17] optimized the synthesis process of DAPO and replaced the triethylamine with sodium hydroxide to increase the DAPO yield to 78%. For research on the DAPO cyclization process, there are few related literature reports, and research on the thermal risk of this process is hardly involved.

This work evaluated the thermal risk of the cyclization process based on a thorough understanding of the cyclization mechanism. First, the cyclization mechanism of DAPO was studied by means of small-scale tests of reactants and reference to relevant literature. Then the exothermic properties were experimentally investigated using a reaction calorimeter (RC1e), and finally, the thermal stability of the materials involved in the cyclization was investigated. This work studied

Received: December 7, 2020
Published: March 2, 2021

https://dx.doi.org/10.1021/acs.oprd.0c00529
Org. Process Res. Dev. 2021, 25, 849–857

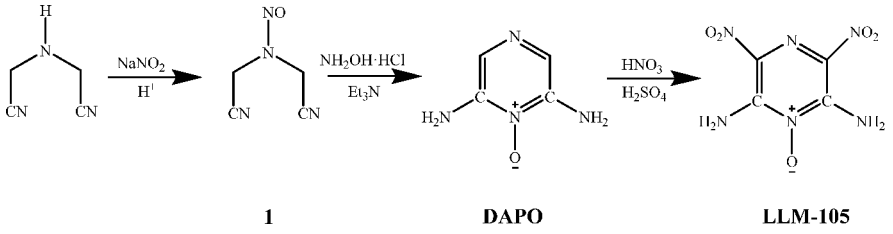

Figure 1. Synthetic method for LLM-105 through a three-step reaction of nitrosation, cyclization and nitration.

Table 1. Specific Operating Conditions for the RC1e tests

run	initially charged mixture	mass of initially charged mixture (g)	mass of hydroxylamine hydrochloride (g)	mass of triethylamine (g)	mole ratio[a]
1	compound **1**/anhydrous methanol	15/118.5	9	26.2 (6.55/6.55/13.1)	1:1:2
2	compound **1**/anhydrous methanol	15/118.5	9	26.2	1:1:2
3	compound **1**/anhydrous methanol	15/118.5	18	26.2	1:2:2
4	anhydrous methanol	118.5	9	26.2 (14.2/12)	1:2

[a]Molar ratio for runs 1, 2, and 3: compound **1**:hydroxylamine hydrochloride:triethylamine. Molar ratio for run 4: hydroxylamine hydrochloride:triethylamine.

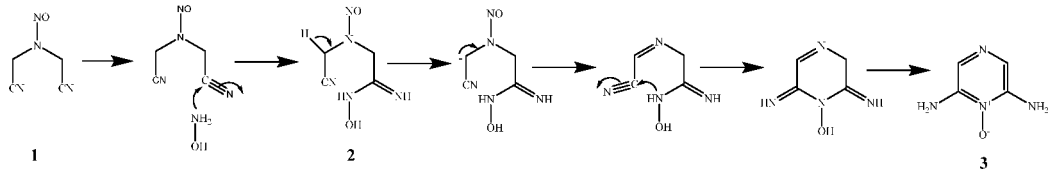

Figure 2. Synthesis mechanism of DAPO.

the thermal risk of the reaction process from the perspective of the reaction mechanism, which can provide a more accurate understanding of the risk of the reaction and improve the accuracy of thermal risk assessment of chemical processes.

2. EXPERIMENT AND APPARATUS

2.1. Reagents. *N*-Nitrosobis(cyanomethyl)amine (98% purity) was purchased from Shanghai Yichun Chemical Technology Co., Ltd. Hydroxylamine hydrochloride (purity 99%) and triethylamine (purity 99%) were purchased from Shanghai Minrell Chemical Technology Co., Ltd. Anhydrous methanol (AR, ≥99.5% purity) was purchased from Sinopharm Chemical Reagent Company. All of the reagents were used without further purification.

2.2. Apparatus. *2.2.1. Reaction Calorimeter.* The RC1e reaction calorimeter used in this work was manufactured by Mettler Toledo and had a 0.5 L glass reactor and an automatic feeding device. The specific operating conditions for the RC1e tests are listed in Table 1.

A total of four runs in the isothermal mode were carried out to characterize the thermal properties of the cyclization reaction. The operation procedures of runs 1, 2, and 3 were as follows: First, anhydrous methanol and compound **1** were added to the reactor at 5 °C. Then hydroxylamine hydrochloride was added, after which triethylamine was slowly dosed with stirring. The reaction mixture was incubated at 5 °C for 30 min and then heated up to 25 °C and allowed to react for 2 h. Postprocessing included filtration, washing, and drying. Triethylamine was dosed through a feeding pump. For run 1, triethylamine was dosed in three portions (6.55, 6.55, and 13.1 g). For runs 2 and 3, triethylamine was continuously dosed to the reactor at one time.

In run 4, anhydrous methanol was added to the reactor without the starting material **1**. At 5 °C, hydroxylamine hydrochloride was added, and then triethylamine was dosed in two portions (14.2 and 12 g).

2.2.2. Differential Scanning Calorimeter. The differential scanning calorimeter (DSC) was manufactured by Mettler Toledo. The samples were sealed in gold-plated high-pressure crucibles (40 μL). For dynamic tests, the heating rates were 2, 4, 8, and 10 K/min, and the temperature range was 30−300 °C. All of the DSC tests were carried out under a high-purity nitrogen atmosphere, and the nitrogen flow rate was 50 mL/min. The DSC crucibles were weighed before and after the tests, and no significant mass loss was observed.

2.2.3. ^{1}H NMR Spectroscopy. ^{1}H NMR spectra were obtained using a Bruker Avance III 500 MHz spectrometer with an ^{1}H sensitivity of ≥650:1 (0.1% EB). The chemical shifts (δ) were reported in parts per million downfield from tetramethylsilane as an internal standard. The solvent was DMSO-d_6. In the ^{1}H NMR spectrum, the characteristic peaks of DMSO and H_2O appear at δ 2.5 and δ 3.3, respectively.

2.2.4. High-Performance Liquid Chromatography. The composition of the product obtained from the RC1e experiment was quantitatively determined by HPLC. The HPLC instrument was produced by Shandong Wukong Instrument Company. The manufacturer of HPLC column is . The chromatographic column used was a Venusil MP C18 column (4.6 mm × 250 mm, 5 μm) (Agela Techonologies Inc., serial number 035843). The solvent system was CH_3OH/CH_3COONH_4 + 0.1% HCOOH, and the flow rate was 1 mL/min. The column temperature was 30 °C, and the absorption wavelength was 254 nm.

2.2.5. Mass Spectrometry Analysis. A Finnigan TSQ Quantum Ultra AM mass spectrometer manufactured by Thermo Fisher Scientific was used to analyze the molecular

https://dx.doi.org/10.1021/acs.oprd.0c00529
Org. Process Res. Dev. 2021, 25, 849−857

weight of the sample. Before the test, the sample was dissolved in anhydrous methanol, and the dissolved sample was filtered with a 0.22 μm microporous membrane.

3. RESULTS AND DISCUSSION

3.1. Research on the Mechanism of the Cyclization Reaction. With respect to the synthesis mechanism of DAPO, on the basis of Harrington's[18] research, Zhao[16] speculated that the synthesis mechanism of DAPO includes three steps in sequence: elimination of −NO, condensation of hydroxylamine, and proton transfer. Triethylamine plays two roles in this reaction: one is to react with hydroxylamine hydrochloride to generate free hydroxylamine, and the other is to remove −NO from compound **2**. Wang[17] experimentally proved that the synthesis of DAPO starts with the condensation reaction of compound **1** and hydroxylamine, not elimination of −NO. Wang proposed the synthesis pathway shown in Figure 2.

To further understand the cyclization processes, three small-scale tests with different molar ratios were carried out. The molar ratios and experimental results are shown in Table 2.

Table 2. Experimental Results with Different Molar Ratios of Reactants

expt	molar ratio[a]	product	yield (%)[b]
1	30:1:1:2	DAPO	60
2	30:1:1:1	**2**	–
3	30:1:2:2	**4**	91

[a]Molar ratio: anhydrous methanol:compound **1**:hydroxylamine hydrochloride:triethylamine. [b]The product yields were calculated as 100% × (molar amount of product)/(molar amount of compound **1**).

When the compound **1**:hydroxylamine hydrochloride:triethylamine molar ratio was 1:1:2, a light-yellow precipitate (Figure 3a) was obtained after the reaction. The ^{1}H NMR results for the precipitate in Figure 4 proved that the precipitate was DAPO. At a molar ratio of 1:1:1, the reaction produced a brown precipitate (Figure 3b). According to the ^{1}H NMR (Figure 5) and mass spectrometry results, this precipitate was verified to be compound **2.** When the molar ratio was 1:2:2, a white precipitate (Figure 3c) was obtained after the reaction. The product was analyzed by HPLC and ^{1}H NMR spectroscopy, as shown in Figure 6. According to ^{1}H NMR analysis, the product was *N*-nitrosoiminodiethylamine oxime (**4**). The yield of compound **4** was ∼91%. The HPLC results indicated that the purity of compound **4** was about 95%. After

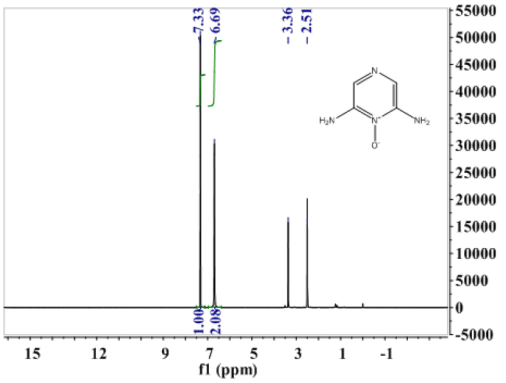

Figure 4. ^{1}H NMR spectrum of DAPO.

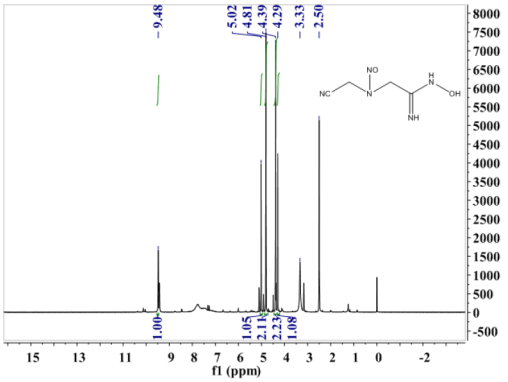

Figure 5. ^{1}H NMR spectrum of compound **2**.

filtration of the reaction mixture, we also used HPLC to test the reaction filtrate. As shown in Figure 6b, this indicated that compound **4** still remained in the reaction filtrate. From the structure of compound **4**, one can conclude that both of the cyano groups in compound **1** condensed with free hydroxylamine, and no elimination reaction occurred. On this basis, the synthesis mechanism of compound **4** shown in Figure 7 is proposed.

On the basis of the above results, one can conclude that the reaction involves two stages. In the first stage, triethylamine reacts with hydroxylamine hydrochloride to produce free hydroxylamine, which then condenses with compound **1** to produce compound **2**. In the second stage, triethylamine catalyzes the removal of the −NO group from compound **2**. If the addition of triethylamine stops before half of the

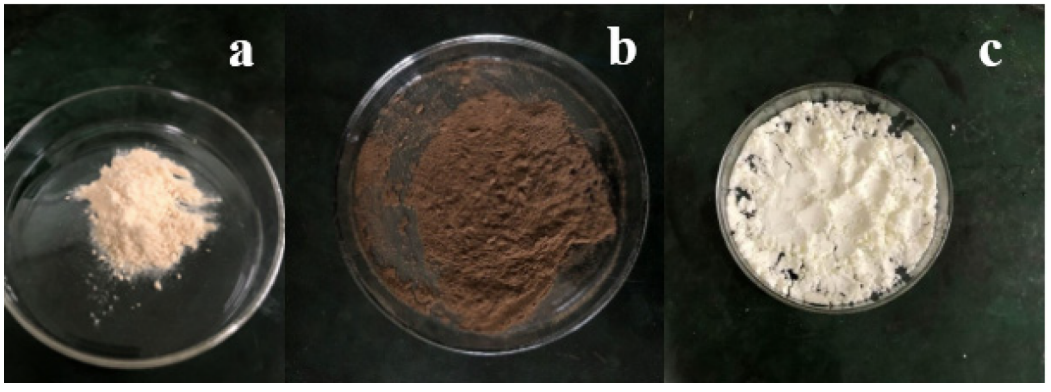

Figure 3. Solid precipitates: (a) DAPO; (b) compound **2**; (c) compound **4**.

https://dx.doi.org/10.1021/acs.oprd.0c00529
Org. Process Res. Dev. 2021, 25, 849−857

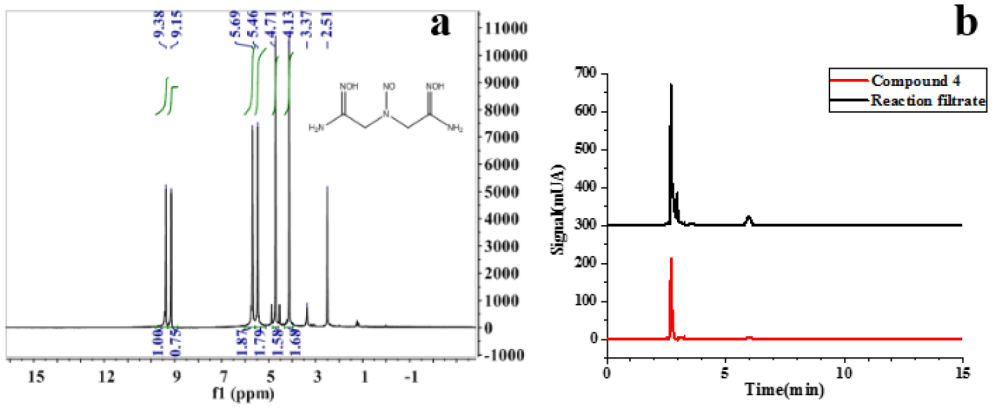

Figure 6. (a) ^{1}H NMR spectrum and (b) HPLC results for compound 4.

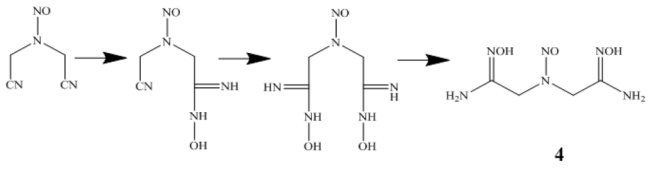

Figure 7. Synthetic mechanism of compound **4**.

triethylamine has been dosed into the reactor, the removal of the −NO group and the cyclization reaction will not happen. This is the case because the triethylamine added will immediately be transformed to triethylamine hydrochloride, which cannot catalyze the subsequent removal of the −NO group and cyclization reaction.

To characterize the reaction rate in the first dosing stage, RC1e run 1 was conducted. The results are shown in Figure 8.

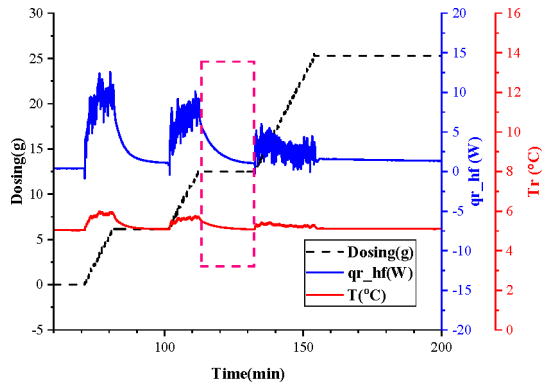

Figure 8. Heat flow profile for run 1.

It can be seen that when the dosing of triethylamine was stopped when half of the triethylamine had been dosed, both the heat flow and the T_r profile gradually decreased. In combination with the result of laboratory-scale experiment 2 in Table 2, one can reasonably expect that in the first dosing stage only the condensation of free hydroxylamine and compound **1** occurs and that the subsequent reactions such as removal of the −NO group and cyclization hardly occur.

Furthermore, after the first dosing stage, the reactions of −NO group removal, proton transfer, cyclization, and rearrangement occur in a continuous way, which means that it is impossible to separate these reactions in the second reaction stage. By integration of the heat flow profile in Figure 8, the heat released in the first dosing stage was obtained as −14.05 kJ (based on compound **1**, the normalized heat was −116.2 kJ/mol).

3.2. Reaction Calorimetry Results. In this section, the thermal features of DAPO synthesis reaction are discussed. The heat flow profiles for runs 2, 3, and 4 are shown in Figures 9−11, respectively, and summarized in Table 3.

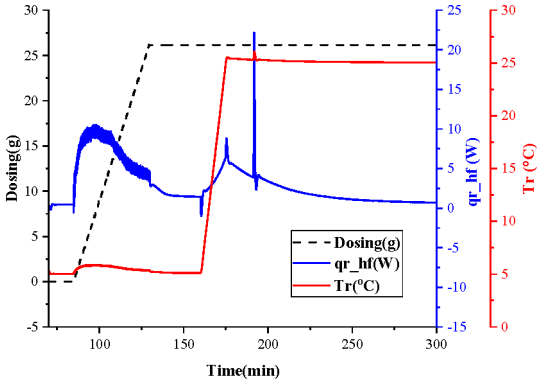

Figure 9. Heat flow and dosing profiles for run 2.

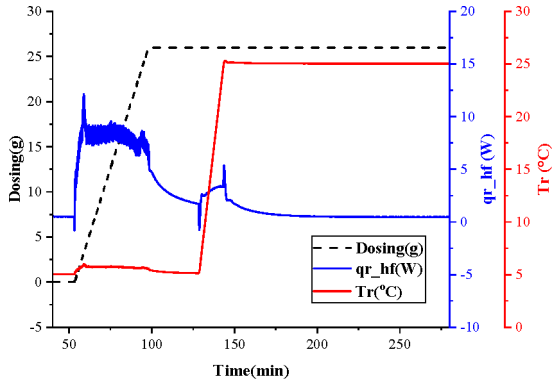

Figure 10. Heat flow and dosing profiles for run 3.

Through integration of the heat flow profiles (Figures 9−11), the total heats (Q_{tot}) generated in runs 2, 3, and 4 were −34, −29, and −2.4 kJ, respectively. In run 3, the compound **1**:hydroxylamine hydrochloride:triethylamine molar ratio was 1:2:2. On the basis of the reaction mechanism discussed in the previous section, both of the cyano groups in compound **1** condensed with the free hydroxylamine to generate compound **4**.

https://dx.doi.org/10.1021/acs.oprd.0c00529
Org. Process Res. Dev. 2021, 25, 849−857

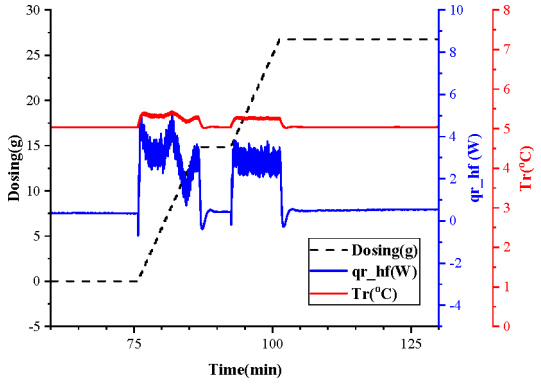

Figure 11. Heat flow and dosing profiles for run 4.

Table 3. RC1 Results for Runs 1−4

run	c_p (J g^{-1} K^{-1})[a]	Q_{tot} (kJ)[b]	ΔT_{ad} (K)
1	2.44	−34	82.6
2	2.44	−34	82.6
3	2.41	−29	67.7
4	2.46	−2.4	6.3

[a]c_p is the specifical heat capacity of the reaction mixture and was obtained by the calibration produced of RC1. [b]For Q, the exotherm is expressed by the minus sign.

With respect to the heat flow profiles in run 4, one can find that the exothermic signals sharply decreased to zero once the dosing event stopped. At first, we considered that the heat released was caused by the neutralization reaction between hydroxylamine hydrochloride and triethylamine. However, this contradicted with the fact that heat was still released after a stoichiometric amount of triethylamine had been added. Then we speculated that the heat released was ascribed to the mixing between triethylamine and methanol. This speculation was experimentally proven by another RC1e run in which triethylamine was dosed into methanol (see the Supporting Information for more details).

3.3. Thermal Stability Analysis of Materials. Thermal stability analysis of the materials involved in the DAPO synthesis process is an essential task for thermal risk assessment. In this section, we discuss the dynamic DSC tests that we employed to quantitatively characterize the thermal stabilities of the materials in stage 1 (condensation of free hydroxylamine) and stage 2 (−NO elimination, cyclization, proton transfer, and rearrangement).

3.3.1. Stage 1. In stage 1, the following materials are involved: compound **1**, a mixture of compound **1** and anhydrous methanol (sample 1), a mixture of compound **1**, anhydrous methanol, and hydroxylamine hydrochloride (sample 2), the final reaction mixture in the first stage (sample 3), and compound **2**. The dynamic DSC results are shown in Figure 12 and Table 4.

From Table 4, one can see that compared with compound **1**, compound **2** has a lower onset temperature (130.1 °C) and higher decomposition heat (−5217.1 J/g), indicating that compound **2** is more thermally risky than compound **1**. Consequently, as shown in Table 4, the onset temperature of sample 3, which contains compound **2**, is lower than those of samples 1 and 2. Furthermore, the decomposition heat of sample 3 is higher than those of samples 1 and 2. Since sample 3 is the most thermally unstable mixture in Table 4, we studied the thermal stability of sample 3 in more detail. Sample 3 was

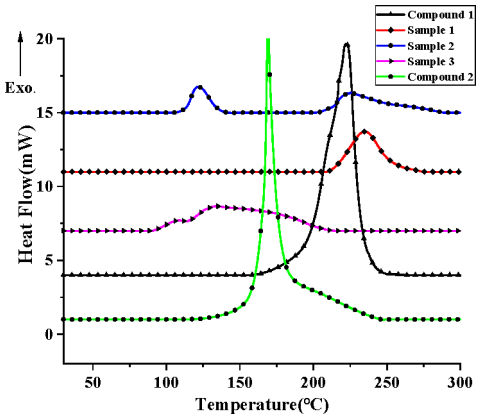

Figure 12. DSC test curves for the related materials in stage 1 at 10 K/min.

Table 4. DSC Test Results for the Related Materials in Stage 1

sample	mass (mg)	T_o (°C)[a]	Q (J/g)[b]
compound **1**	0.77	163.2	−2899.0
sample1	3.70	205.3	−117.2
sample 2	2.65	105.2	−73.5
sample 3	3.55	90.6	−198.5
compound **2**	0.34	130.1	−5217.1

[a]Onset temperature (i.e., the temperature at which the exothermic peak deviates from the baseline). [b]Decomposition heat.

tested by dynamic DSC experiments at four different heating rates. The dynamic DSC heat flow profiles and results for sample 3 are shown in Figure 13 and Table 5.

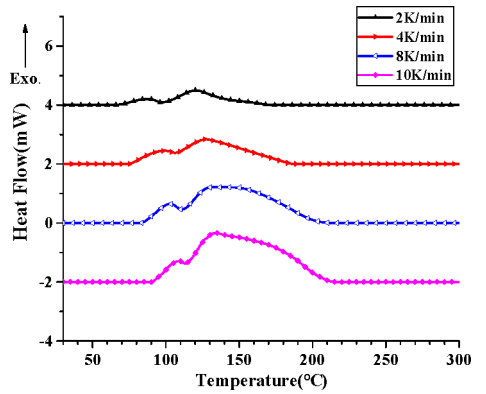

Figure 13. DSC test results for sample 3 at different heating rates.

In Figure 13, one can see that the decomposition of sample 3 contains two overlapped processes. The onset temperature of the first process ranged from 65.5 to 90.6 °C. The average

Table 5. Dynamic DSC Test Results for Sample 3

β (K/min)[a]	mass (mg)	T_o (°C)[b]	Q (J/g)[c]
2	3.52	65.5	−176.0
4	3.54	75.6	−206.3
8	3.50	83.2	−186.8
10	3.55	90.6	−198.5

[a]Heating rate. [b]Onset temperature (i.e., the temperature at which the exothermic peak deviates from the baseline). [c]Decomposition heat.

https://dx.doi.org/10.1021/acs.oprd.0c00529
Org. Process Res. Dev. 2021, 25, 849−857

decomposition heat of sample 3 was −191.9 J/g. To conduct kinetic analysis of the decomposition process of sample 3 in Figure 13, the Friedman method was employed.[19] The Friedman method is a model-free method whose basic equation is shown in eq 1:

$$\ln\left(\frac{d\alpha}{dt}\right)_\alpha = \ln[f(\alpha)A_\alpha] - \frac{E_\alpha}{RT_\alpha} \quad (1)$$

where $d\alpha/dt$ is the reaction rate (in s^{-1}), α is the conversion, A_α is the pre-exponential factor at reaction conversion α (in s^{-1}), $f(\alpha)$ is the reaction model,; E_α is the activation energy (in kJ/mol), R is the ideal gas constant (8.314 J mol^{-1} K^{-1}), and T is the temperature (in K).

In the adiabatic system, the heat released by the sample is completely used for the temperature rise of the sample itself, that is,

$$c_p' m\frac{dT}{dt} = Q\frac{d\alpha}{dt} \quad (2)$$

where m is the sample mass and c_p' is the specific heat capacity of the sample. Because

$$\Delta T_{ad}' = \frac{Q}{mc_p'} \quad (3)$$

where $\Delta T_{ad}'$ is the adiabatic temperature rise of the material when the thermal inertia factor (φ) is equal to 1, it follows that for $\varphi = 1$,

$$\frac{dT}{dt} = \Delta T_{ad}'\frac{d\alpha}{dt} \quad (4)$$

For $\varphi \neq 1$, eq 4 can be expressed as

$$\frac{dT}{dt} = \frac{1}{\varphi}\Delta T_{ad}'\frac{d\alpha}{dt} \quad (5)$$

Equation 1 for the reaction rate can be rearranged to

$$\frac{d\alpha}{dt} = f(\alpha)A_\alpha \exp\left(-\frac{E_\alpha}{RT_\alpha}\right) \quad (6)$$

By the use of eqs 4 and 5, eq 6 can be transformed into

$$\frac{dT}{dt} = \Delta T_{ad}' f(\alpha)A_\alpha \exp\left(-\frac{E_\alpha}{RT_\alpha}\right) \quad (7)$$

$$\frac{dT}{dt} = \frac{1}{\varphi}\Delta T_{ad}' f(\alpha)A_\alpha \exp\left(-\frac{E_\alpha}{RT_\alpha}\right) \quad (8)$$

respectively. The time under adiabatic conditions can be obtained using the following equation:

$$t_\alpha = \int_0^{t_\alpha} dt = \int_0^{t_\alpha} \frac{d\alpha}{f(\alpha)A_\alpha \exp\left(-\frac{E_\alpha}{RT_\alpha}\right)} \quad (9)$$

for $\alpha \in [0, 1]$. Since the Friedman method gives the relationship between $\ln[f(\alpha)A_\alpha]$ and E_α at conversion α, the relationship between the temperature rise rate at a certain conversion rate can be obtained according to eq 7 or eq 8. Combining this with eq 9, one can obtain the temperature rise rate versus time curve at any starting temperature, from which the relationship between the time to maximum rate under adiabatic conditions (TMR_{ad}) and the starting temperature T can be obtained.

The comparison between the experimental and simulated reaction progress profiles is shown in Figure 14. The

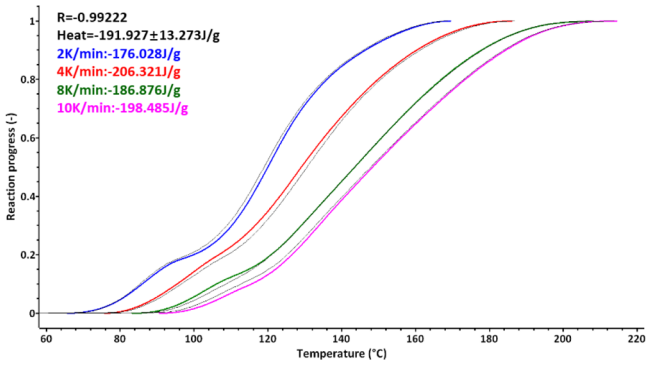

Figure 14. Comparison between the experimental and simulated reaction progress profiles for sample 3.

correlation coefficient R in Figure 14 is higher than 0.99, which proves the validation of the simulated results. On the basis of the above kinetic analysis results, we then predicted the trend of TMR_{ad},[20−22] as shown in Figure 15. From Figure 15, one can directly read that T_{D24}, which is the temperature corresponding to TMR_{ad} for 24 h, is equal to 31.1 °C.

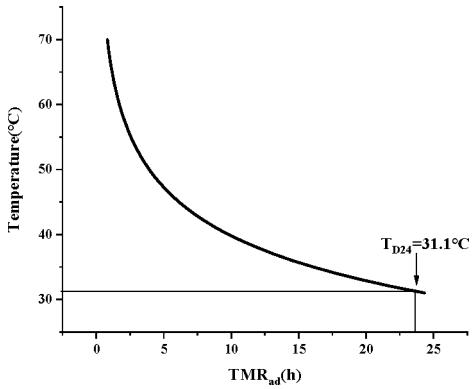

Figure 15. TMR_{ad} prediction curve for sample 3.

3.3.2. Stage 2. Dynamic DSC experiments were also performed on three materials involved in stage 2: the final reaction mixture (sample 4), DAPO, and compound **4**. The results are shown in Figure 16 and summarized in Table 6. The heat flow curve for sample 4 has two separate exothermic peaks. The first exothermic peak starts at 121.2 °C, and the decomposition heat for this peak was obtained as −203.8 J/g. From Table 6, one can find that compound **4**, as a side product in the DAPO synthesis process, presents a more risky nature than the target product DAPO. The exothermic peak of compound **4** in Figure 16 appears in the same temperature range as the first peak of sample 4, indicating that the first exothermic peak of sample 4 can be ascribed to the decomposition of compound **4** (the presence of compound **4** was confirmed by HPLC analysis). The second exothermic peak of sample 4 corresponds to the decomposition of the target compound DAPO.

Since sample 4 presented the lowest exotherm onset temperature in Table 6, we conducted more dynamic DSC tests on sample 4. The results are shown in Figure 17 and summarized in Table 7.

https://dx.doi.org/10.1021/acs.oprd.0c00529
Org. Process Res. Dev. 2021, 25, 849−857

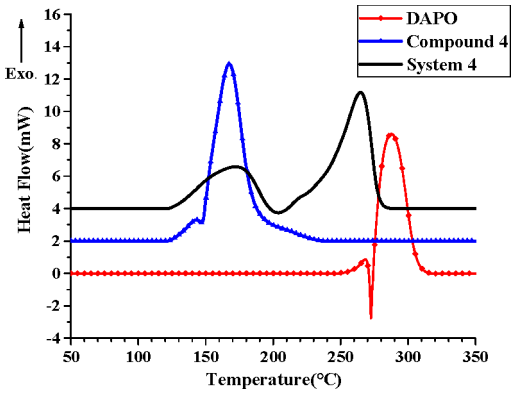

Figure 16. DSC test curves for the related materials in stage 2 at 10 K/min.

Table 6. DSC Test Results for the Related Materials in Stage 2

sample	mass (mg)	T_o (°C)[a]	Q (J/g)[b]
sample 4	3.82	121.2	−649.28
DAPO	0.72	248.2	−1353.3
compound **4**	0.88	121.6	−3565.9

[a]Onset temperature (i.e., the temperature at which the exothermic peak deviates from the baseline). [b]Decomposition heat.

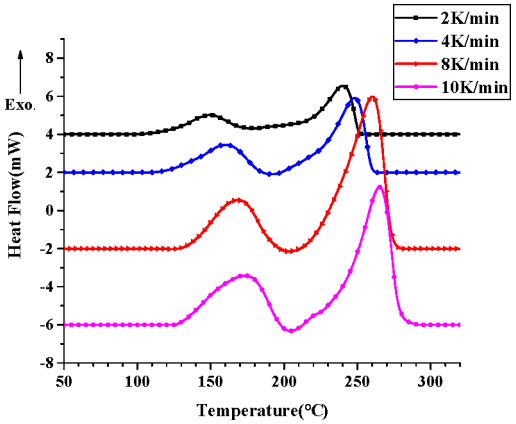

Figure 17. DSC test results for sample 4 at different heating rates.

Table 7. Dynamic DSC Test Results for Sample 4

β (K/min)[a]	mass (mg)	T_o (°C)[b]	Q′ (J/g)[c]
2	3.82	101.4	−205.5
4	3.79	110.8	−205.2
8	3.78	119.6	−196.4
10	3.82	121.2	−203.8

[a]Heating rate. [b]Onset temperature (i.e., the temperature at which the exothermic peak deviates from the baseline). [c]Decomposition heat for the first exothermic peak of sample 4.

The two exothermic peaks in Figure 17 are separated completely. One can reasonably expect that when a thermal runaway event occurs, the first exothermic peak will be triggered first. Hence, to calculate the safety parameters of TMR_{ad}, the kinetic calculation focused only on the first exothermic peak. The value of the correlation coefficient R in Figure 18 illustrates the validity of the fitting results. The TMR_{ad} prediction curve for sample 4 is shown in Figure 19 and gives a T_{D24} of 69.4 °C.

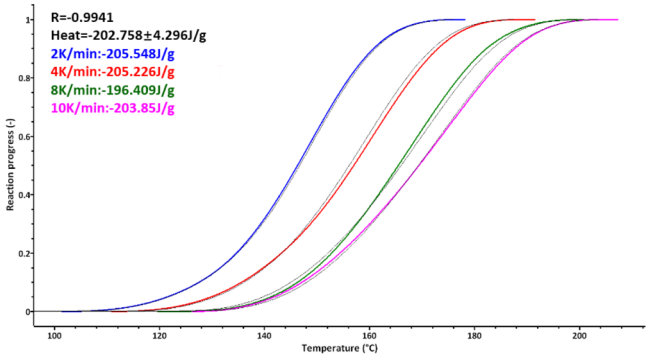

Figure 18. Comparison between the experimental and simulated reaction progress profiles for sample 4.

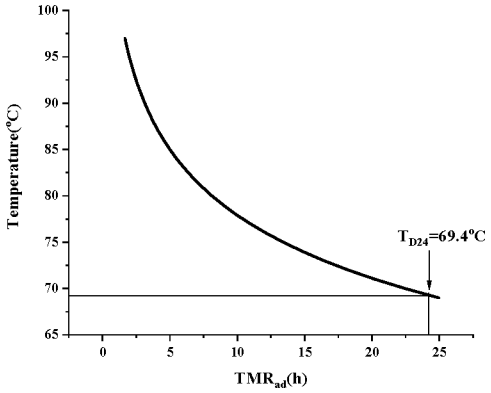

Figure 19. TMR_{ad} prediction curve for sample 4.

3.4. Thermal Risk Analysis. In order to better understand the consequences of insufficient cooling capacity, it is necessary to calculate the maximum temperature that the reaction system can reach under adiabatic conditions (MTSR) by calculating the heat accumulated after the target reaction runs away during the dosing process.[23−25] The acquisition of the MTSR is related to the maximum temperature that can be reached at any time if the reaction runs away (T_{cf}):[26]

$$\mathrm{MTSR} = \max(T_{cf}) = T_r + \Delta T_{ad} X_{ac,max} \frac{M_{rf}}{M_{r,max}} \tag{10}$$

where T_r is the temperature of the reaction system before cooling failure (which can be considered as the process temperature), ΔT_{ad} is the adiabatic temperature rise caused by heat accumulation, $X_{ac,max}$ is the maximum thermal accumulation of the unreacted reactant, M_{rf} is the mass of the reaction mixture at the end of dosing, and $M_{r,max}$ is the mass of the reaction mixture at the maximum accumulation.

3.4.1. Stage 1. From the RC1e result for run 1, the heat generated in stage 1 was obtained as 14.05 kJ. The adiabatic temperature rise ΔT_{ad} at this stage can be calculated as follows:

$$\Delta T_{ad} = \frac{Q_{tot}}{mc_p} \tag{11}$$

where m is the mass of the entire reaction mixture added to the reactor and c_p is the specific heat capacity of the reaction mixture. For stage 1,

https://dx.doi.org/10.1021/acs.oprd.0c00529
Org. Process Res. Dev. 2021, 25, 849−857

$$\Delta T_{ad} = \frac{14.05 \times 10^3}{155.6 \times 2.44} = 37\ \text{K} \quad (12)$$

Furthermore, by integration of the heat flow profile for run 2, the heat produced before the addition of half of the triethylamine was found to be 11.2 kJ. Thus, the heat accumulated in the reaction mixture for stage 1 was

$$Q_{ac} = 14.05 - 11.2 = 2.85\ \text{kJ} \quad (13)$$

The thermal accumulation for run 3 was:

$$X_{ac,max} = \frac{2.85}{14.05} = 20.3\% \quad (14)$$

Consequently, using eq 10 we can calculate the MTSR value for stage 1, which is equal to 12.5 °C.

The above analysis shows that the MTSR (12.5 °C) is less than the T_{D24} (31.1 °C), which means that in the case of cooling failure, immediately stopping the addition of triethylamine will not cause secondary decomposition of the reaction mixture.

3.4.2. Stage 2. For stage 2, the reaction temperature is increased from 5 to 25 °C. This process is non-isothermal, and the MTSR is calculated as follows:

At the end of the triethylamine addition, the heat accumulation of the material is the largest, and by integration of the heat flow profile of run 2, the heat conversion rate at this time is about 55.8%. Thus, the MTSR at this time point is calculated to be

$$\begin{aligned} \text{MTSR}_{5^\circ\text{C}} &= T_p + \frac{Q}{mc_p} X_{ac} \\ &= 5 + \frac{34 \times 10^3}{168.7 \times 2.44} \times (1 - 0.558) \\ &= 41.5\ ^\circ\text{C} \end{aligned} \quad (15)$$

When the temperature increased to T_p = 25 °C, about 70.3% of the heat was released. Thus, the MTSR at 25 °C can be obtained as

$$\begin{aligned} \text{MTSR}_{25^\circ\text{C}} &= T_p + \frac{Q}{mc_p} X_{ac} \\ &= 25 + \frac{34 \times 10^3}{168.7 \times 2.44} \times (1 - 0.703) \\ &= 49.5\ ^\circ\text{C} \end{aligned} \quad (16)$$

On the basis of the above calculations, the MTSR of stage 2 is determined to be 49.5 °C. The MTSR (49.5 °C) is lower than T_{D24} (69.4 °C), which means that in the case of a cooling failure, immediately stopping the addition of triethylamine will not cause the secondary decomposition. However, if all of the triethylamine is accidentally dosed to the reactor in a short time, the MTSR can be approximated as the sum of T_p and ΔT_{ad}, given by

$$\text{MTSR} = T_p + \Delta T_{ad} = 5 + \frac{34 \times 10^3}{168.7 \times 2.44} = 87.6\ ^\circ\text{C}$$

In this case, the MTSR is higher than T_{D24} (69.4 °C), indicating that decomposition of the reaction mixture will be triggered. Therefore, from the safety point of view, the dosing rate of triethylamine must be effectively controlled to avoid accumulation of reactants. Otherwise, the practical value of the MTSR could be higher than the MTSR obtained in this work and could surpass the T_{D24} of 69.4 °C, potentially leading to higher safety risks.

4. CONCLUSION

A thermal risk assessment of DAPO synthesis based on a study of the reaction mechanism has been carried out. The following conclusions were obtained:

(1) In the first dosing stage, only the condensation of free hydroxylamine and compound **1** occurs; in the second dosing stage, the subsequent reactions such as removal of the −NO group and cyclization occur. If the dosing stopped in the first stage, the reactions involved in the second stage hardly occur.

(2) The main intermediate product in the first dosing stage is compound **2**, and the main side product in the DAPO synthesis process has been proven to be compound **4**.

(3) Dynamic DSC tests revealed that both intermediate **2** and side product **4** are more thermally risky than the target compound DAPO.

(4) Thermal risk analysis showed that a thermal runaway incident can be avoided as long as the dosing is stopped immediately after the cooling failure event occurs.

■ ASSOCIATED CONTENT

Supporting Information

The Supporting Information is available free of charge at https://pubs.acs.org/doi/10.1021/acs.oprd.0c00529.

Mass spectrum profiles for **2**, calorimetry test result to measure the heat of mixing for trimethylamine and methanol, profiles of E and $\ln[f(\alpha)A_\alpha]$ versus α for samples 3 and 4, and HPLC profiles of side product **4** and the reaction filtrate obtained in run 2 (the product liquid after DAPO was filtered out) (PDF)

■ AUTHOR INFORMATION

Corresponding Author

Zichao Guo − *Department of Safety Engineering, School of Chemical Engineering, Nanjing University of Science and Technology, Nanjing, Jiangsu 210094, China*; orcid.org/0000-0002-2288-1174; Phone: +86 025 84315526; Email: gzc319@njust.edu.cn; Fax: +86 025 84315526

Authors

Yuehua Li − *Department of Safety Engineering, School of Chemical Engineering, Nanjing University of Science and Technology, Nanjing, Jiangsu 210094, China*

Yang Wang − *Department of Safety Engineering, School of Chemical Engineering, Nanjing University of Science and Technology, Nanjing, Jiangsu 210094, China*

Longyu Liao − *Institute of Chemical Materials, China Academy of Engineering Physics, Mianyang 621999, China*

Liping Chen − *Department of Safety Engineering, School of Chemical Engineering, Nanjing University of Science and Technology, Nanjing, Jiangsu 210094, China*

Wenqian Wu − *Department of Safety Engineering, School of Chemical Engineering, Nanjing University of Science and Technology, Nanjing, Jiangsu 210094, China*

Complete contact information is available at: https://pubs.acs.org/10.1021/acs.oprd.0c00529

https://dx.doi.org/10.1021/acs.oprd.0c00529
Org. Process Res. Dev. 2021, 25, 849−857

Notes

The authors declare no competing financial interest.

■ ACKNOWLEDGMENTS

The authors thank Dr. Shi Mingyang for the ^{1}H NMR tests and Dr. Li Xin for his help in formation heat calculation. This work was financially supported by the National Key R&D Program of China (2017YFC0804701-4) and the Opening Project of the Key Laboratory of Special Energy Materials (Nanjing University of Science and Technology), Ministry of Education, China.

■ REFERENCES

(1) Pagoria, P. F. Synthesis, Scale-Up, and Characterization of 2,6-diamino-3,5-dinitropyrazine-1-oxide (LLM-105). *Propellants, Explos., Pyrotech.* **1998**, *23*, 156−160.
(2) Cutting, J. L.; Chau, H. H.; Peng, H. P. A Small-Scale Screening Test for HE Performance: Application to the New Explosive LLM-105. *Pyrotech. Intell.* **2001**, *2*, 45−53.
(3) Pagoria, P. F. Synthesis of high explosive. UCID 220622297, 1997.
(4) Alós, M. A.; Strozzi, F.; Zaldívar, J. M. A New Method for Assessing the Thermal Stability of Semi-Batch Processes Based on Lyapunov Exponents. *Chem. Eng. Sci.* **1996**, *51*, 3089−3094.
(5) Zaldívar, J. M.; Molga, E.; Alós, M. A.; Hernández, H.; Westerterp, K. R. Aromatic Nitrations by Mixed Acid. Fast Liquid-Liquid Reaction Regime. *Chem. Eng. Process.* **1996**, *35*, 91−105.
(6) Zaldívar, J. M.; Barcons, C.; Hernandez, H.; Molga, E.; Snee, T. J. Modelling and Optimization of Semi-Batch Toluene Mononitration with Mixed Acid from Performance and Safety Viewpoints. *Chem. Eng. Sci.* **1992**, *47*, 2517−2522.
(7) Zaldívar, J. M.; Molga, E.; Alós, M. A.; Hernandez, H.; Westerterp, K. R. Aromatic Nitrations by Mixed Acid. Slow Liquid-Liquid Reaction Regime. *Chem. Eng. Process.* **1995**, *34*, 543−559.
(8) D'angelo, F. A.; Brunet, L.; Cognet, P.; Cabassud, M. Modeling and Constraint Optimization of an Aromatic Nitration in Liquid-Liquid Medium. *Chem. Eng. J.* **2003**, *91*, 75−84.
(9) Bellamy, A. J.; Golding, P. The Study of Some Potential New Synthetic Routes to LLM-105 (2,6-Diamino-3,5-dinitropyrazine 1-oxide). *Cent. Eur. J. Energy Mater.* **2007**, *4*, 33−57.
(10) Shaw, J. T.; Brotherton, C. E.; Moon, R. W.; Winland, M. D.; Anderson, M. D.; Kyler, K. S. The Preparation of 2,6-Diaminopyrazine, 2,6-Diazidopyrazine and Some of Their Derivatives. *J. Heterocycl. Chem.* **1980**, *17*, 11−16.
(11) Ritter, H.; Licht, H. H. Synthesis and Reactions of Dinitrated Amino and Diaminopyridines. *J. Heterocycl. Chem.* **1995**, *32*, 585−590.
(12) Hollins, A.; Merwin, L. H.; Nissan, R. A.; Wilson, W. S.; Gilardi, R. Aminonitropyridines and their N-Oxides. *J. Heterocycl. Chem.* **1996**, *33*, 895−904.
(13) Yu, X. Y.; Lu, M.; Nie, F. D. Improvement of the Synthesis Process of 2,6-Diamino-3,5-Dinitropyrazine-1-Oxide. *Chin. J. Explos. Propellants* **2012**, *35*, 10−10.
(14) Li, Y.; Huang, F. C.; Wang, Y. B.; Hu, L. L.; Zhang, M. M.; Zhou, W. J. Research Progress on Synthesis and Application of 2,6-Diamino-3,5-dinitropyrazine-1-oxide. *Chem. World* **2017**, *1*, 57−64.
(15) Pagoria, P. F.; Zhang, X. M. Synthesis of Pyrazines Including 2,6-Diaminopyrazine-1-oxide (DAPO) and 2,6-Diamino-3,5-dinitropyrazine-1-oxide (LLM-105). WO 2010/123806 A1, 2010.
(16) Zhao, X. F.; Liu, Z. L.; Yao, Q. Z.; Cheng, J.; Dong, Y. Synthesis of 2,6-Diamino-3,5-dinitropyrazine-1-oxide. *Chin. J. Explos. Propellants* **2012**, *35*, 15−17.
(17) Wang, J. M.; Du, Y. Optimization of Synthetic Method of 2,6-Diamino-pyrazine-1-oxide. *Chin. J. Explos. Propellants* **2017**, *40*, 25−27.
(18) Vohra, S. K.; Harrington, G. W.; Zacharias, D. E.; Swern, D. New Synthesis of 2-Amino-6-Alkoxypyrazines from N-Nitrosobis-(cyanomethyl)amine and Alkoxides. *J. Org. Chem.* **1979**, *44*, 1128−1130.
(19) Friedman, H. L. Kinetics of Thermal Degradation of Char-forming Plastics from Thermogravimetry. *J. Polym. Sci., Part C: Polym. Symp.* **1964**, *6*, 183−195.
(20) Wu, D. J.; Qian, X. M. Experimental Study on the Thermal Runaway of Hydrogen Peroxide with In-/Organic Impurities by a Batch-Reactor. *J. Loss Prev. Process Ind.* **2018**, *51*, 200−207.
(21) Wang, Z.; Richter, S. M.; Gates, B. D.; Grieme, T. A. Safety Concerns in a Pharmaceutical Manufacturing Process Using Dimethyl Sulfoxide (DMSO) as a Solvent. *Org. Process Res. Dev.* **2012**, *16*, 1994−2000.
(22) Vernieres-Hassimi, L.; Dakkoune, A.; Abdelouahed, L.; Estel, L.; Leveneur, S. Zero-Order versus Intrinsic Kinetics for the Determination of the Time to Maximum Rate under Adiabatic Conditions (TMR_{ad}): Application to the Decomposition of Hydrogen Peroxide. *Ind. Eng. Chem. Res.* **2017**, *56*, 13040−13049.
(23) Guo, Z. C.; Li, S. R.; Zhou, P.; Chen, L. P.; Chen, W. H. Insights into Maximum Temperature of Synthesis Reactions in Isothermal Homogeneous Semi-Batch Reactors. *Thermochim. Acta* **2018**, *668*, 103−109.
(24) Shah, S.; Fischer, U.; Hungerbühler, K. Assessment of Chemical Process Hazards in Early Design Stages. *J. Loss Prev. Process Ind.* **2005**, *18*, 335−352.
(25) Zhang, L.; Yu, W. D.; Pan, X. H.; Fang, J. J.; Hua, M.; Chen, F. M.; Jiang, J. C. Thermal Hazard Assessment for Synthesis of 3-Methylpyridine-*N*-Oxide. *J. Loss Prev. Process Ind.* **2015**, *35*, 316−320.
(26) Stoessel, F. *Thermal Safety of Chemical Processes: Risk Assessment and Process Design*; Wiley-VCH: Weinheim, Germany, 2008.

https://dx.doi.org/10.1021/acs.oprd.0c00529
Org. Process Res. Dev. 2021, 25, 849−857